The dielectric response of water in high electric fields: equilibrium water thickness and the field distribution

Dawn L. Scovell, Tim D. Pinkerton, Bruce A. Finlayson, Eric M. Stuve *

University of Washington, Department of Chemical Engineering, Box 351750, Seattle, WA 98195, USA

Received 7 May 1998; in final form 28 July 1998

Abstract

Adsorption and reaction of water at metal surfaces can be strongly influenced by high surface electric fields. A numerical model, which includes a field-dependent relative permittivity of water, has been developed to predict the equilibrium thickness of the condensed water layer and its effect on the field distribution around a field emitter tip. Thin water layers weaken the field at the tip surface while thick layers concentrate it. When the water becomes sufficiently thick, the field at the tip surface becomes greater than the field at a clean tip surface for the same applied potential.

1. Introduction

Understanding the dielectric response of water is key to predicting the behavior of water in high electric fields. This is especially true when predicting how the presence of water affects the electric field distribution at an electrode surface. It is usually assumed that large fields on the order of 1 V $Å^{-1}$ exist at the electrode surfaces in electrochemical cells [1], but little is actually known about how water affects the electric field distribution.

A field emitter tip lends itself to studying the dielectric properties of water because it produces fields sufficiently large to cause condensation [2–8]. Condensed water can form on a field emitter tip at partial pressures of water as low as 10^{-8} Torr [5]. An advantage of studying water on field emitter tips is that all parameters that affect the condensation point, i.e., temperature, water partial pressure and applied field, can be independently controlled. A complication with this approach is that the water adlayer thickness and the electric field strength depend upon each other.

As a first step in understanding the effect of high electric fields on the dielectric behavior of water, we have conducted numerical analyses to quantify the effects of water on the electric field distribution around an emitter tip. The field distribution calculations are novel in that they include a field-dependent relative permittivity for the water adlayer. The model includes determination of the conditions at which water will condense, the effect of condensed water on the electric field distribution, and a prediction of the equilibrium thickness of the water adlayer.

2. Field enhanced condensation

When a dipole, such as water, is placed in an electric field an attractive interaction develops

* Corresponding author. E-mail: stuve@u.washington.edu

through the permanent and induced dipole moments [9]. As a result, the effective pressure of the gas in the high-field region surrounding a field emitter tip is enhanced and water can condense on the tip, as illustrated in Fig. 1. Layers of condensed water start to form on a tip when the adsorption rate exceeds the desorption rate. The enhanced pressure around the tip increases the rate at which gas molecules strike it. If the tip and gas temperatures are equal and if diffusion up the shank is ignored, then the rate at which molecules arrive at a spherical tip is [10]:

$$\dot{N}_{w,a} = \frac{P_\infty}{\sqrt{2\pi mkT}}\left[\exp(-\phi) + \sqrt{\pi\phi}\,\mathrm{erf}\left(\sqrt{\phi}\right)\right], \quad (1)$$

where P_∞ is the pressure far from the tip, m the molecular mass, k the Boltzmann constant, T temperature, ϕ the ratio of polarization and thermal energy $\phi = (\mu E + \frac{1}{2}\alpha E^2)/kT$, E the electric field, μ the dipole moment, α the polarizability, and $\mathrm{erf}(x)$ the error function given by $\mathrm{erf}(x) = 2(\pi)^{-1/2}\int_0^x e^{-t^2}\,dt$. The rate at which molecules desorb from a surface depends upon the frequency of attempts and the energy required to leave the surface:

$$\dot{N}_{w,d} = \nu N_w \exp\left[\frac{-(\Delta U^\circ_{des})}{kT} - \phi\right], \quad (2)$$

where ν is the attempt frequency, N_w the surface density of water molecules and ΔU°_{des} the activation energy for desorption in the absence of an applied field. Eq. (2) assumes that there is no preferential ordering of the dipoles in the condensed layer and that the vapor pressure enhancement due to the curved surface is negligible. This latter assumption is reasonable because the vapor pressure of water is increased by less than 3% for a field emitter tip with a radius of 400 Å.

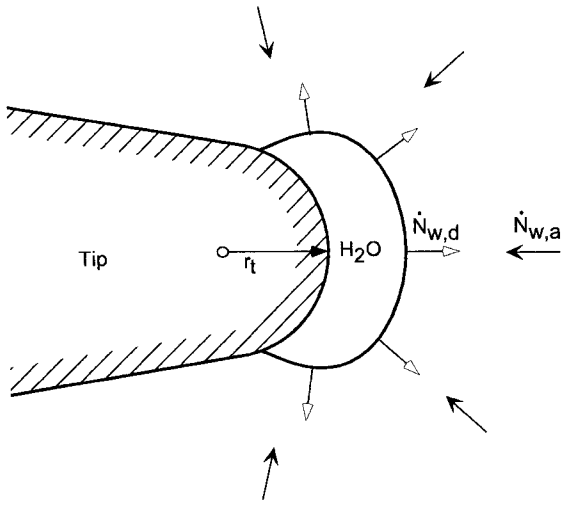

Fig. 1. Condensed water on a field emitter tip with radius r_t will form when the adsorption rate $\dot{N}_{w,a}$ exceeds the desorption rate $\dot{N}_{w,d}$.

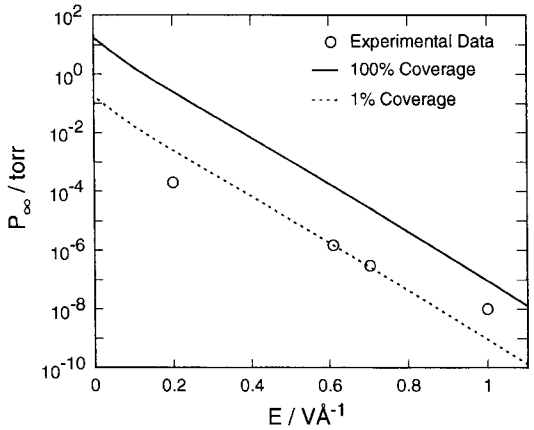

Fig. 2. Partial pressure of water P_∞ at onset of condensation as a function of field strength E. The circles are experimental data from Table 1, the solid line represents formation of a complete monolayer on the surface, and the dashed line represents formation of 1% of a monolayer. The tip and gas temperatures are both 293 K.

The chamber pressure (far from the tip) at which water condenses for a given field E can be calculated by equating the adsorption and desorption rates and solving for P_∞. The field-condensation pressure for water at 293 K is shown by the solid line in Fig. 2 for $\mu = 6.1 \times 10^{-30}$ C m [11] and $\alpha = 1.6 \times 10^{-40}$ $C^2\ m^2\ J^{-1}$ [12]; these values are for gas-phase water. In the absence of an applied field, condensation occurs when P_∞ equals or exceeds the saturation pressure of water, which is 17.5 Torr at 293 K [12].

It is well known that high electric fields enhance the onset of water condensation [2–8]. Water usually forms H_2O^+ and $(H_2O)_n \cdot H^+$ ions, where n varies from 1 to 10. The formation of ionic clusters occurs in multilayers of water molecules [2]. Several groups have investigated the conditions at which protonated water clusters desorb from a field emitter tip at room temperature. The conditions at which ionic clusters have been detected are summarized in Table 1.

Table 1
Summary of empirical data of field-enhanced water condensation at room temperature

Substrate	Field (V Å^{-1})	P_∞ (10^{-6} Torr)	n_{max}	Ref.
W	0.2	100	4	[4]
W	0.2	100–440	3	[7]
Pt	0.61	1.5–500	2	[7]
Pt	0.7	0.3	1	[13]
Rh	1.0	0.01	1	[5]

Fig. 2 compares the minimum field-condensation pressures in Table 1 to those calculated by equating the adsorption and desorption rates. The experimentally observed pressures are considerably lower than those predicted by Eq. (2). One possible explanation for this is that ionic clusters desorb before a complete monolayer of water exists. Several experimental observations support this hypothesis. First, the field at the onset of ionization shows a strong substrate dependence, which would not be expected for the case of multilayers of water. Second, Schmidt found that the onset field for ionization did not change as pressure increased [7]. As we will discuss in Section 4, we only expect this to be true for partial surface coverage because once a complete monolayer forms, the onset field for ionization should increase as pressure increases. Finally, Schmidt found that increasing pressure produced more ionic clusters at constant field strength [7]. If the trapping probability is the same on a bare surface as it is on a water-covered surface, then for $\dot{N}_{w,a} < \dot{N}_{w,d}$ the amount of adsorbed water can be approximated as [10]:

$$\theta = \dot{N}_{w,a}/\dot{N}_{w,d}. \tag{3}$$

This expression predicts that the surface coverage of water increases with pressure because $\dot{N}_{w,a}$ is linear in pressure. If the number of ions that desorb from the surface is proportional to the surface coverage, then the number of desorbing ions will increase as the partial pressure of water increases.

The dashed line in Fig. 2 represents the conditions at which 1% of the surface is covered by water when the adsorption energy is the same for both adsorption to the tip surface and adsorption to multilayer water. The predicted pressures are approximately the same order of magnitude as the minimum pressures at which ionic clusters first appear. Infrared spectroscopy supports the feasibility of forming water clusters at low surface coverage. For example, Griffiths et al. report that even at low coverage (i.e., their detection limit) every water molecule on a Pt(100)-hex or -(1×1) surface is involved in a cluster [14]. Therefore, it is reasonable to assume that ionic clusters form at 1% surface coverage and that the dashed line in Fig. 2 is representative of the conditions at which water clusters are first observed. If this is true, then the solid line in Fig. 2 can be used to estimate the conditions at which a complete monolayer of water forms on the surface.

3. Field distribution

The presence of a high dielectric material, such as water, on an emitter tip changes the electric field distribution around the tip significantly. The effect of condensed water on the electric field distribution can be calculated by assuming that: the tip can be approximated as a spherical, perfect conductor; water does not react with the substrate; macroscopic properties apply; and water ionization is negligible. With these assumptions the potential ψ can be found by solving Poisson's equation

$$\frac{d^2\psi}{dr^2} + \left[\frac{2}{r} + \frac{1}{\varepsilon(E)}\frac{d\varepsilon(E)}{dr}\right]\frac{d\psi}{dr} = 0 \tag{4}$$

for the water layer and Laplace's equation

$$\frac{d^2\psi}{dr^2} + \frac{2}{r}\frac{d\psi}{dr} = 0 \tag{5}$$

for the gas outside the water layer, where r is radial distance, and ε the relative permittivity. The boundary conditions are:

1. the potential at the tip surface: ψ_t,
2. equality of potential at the water/vacuum interface: $\psi_w|_{r=r_w} = \psi_v|_{r=r_w}$,
3. equality of electric displacement at the water/vacuum interface:

$$\varepsilon(E_w)\left.\frac{d\psi_w}{dr}\right|_{r=r_w} = \left.\frac{d\psi_v}{dr}\right|_{r=r_w},$$

and

4. zero potential infinitely far from the tip ($\psi|_{r=\infty} = 0$),

where the subscripts w and v refer to water and vacuum, respectively.

The relative permittivity of the water adlayer is a strong function of field strength. At field strengths of $< 10^{-3}$ V Å^{-1} the relative permittivity changes only slightly with field and has been characterized with the following empirical relationship [15]:

$$\varepsilon = 80 - 10^5 \left(E/\mathrm{V\,\mathring{A}^{-1}} \right)^2 . \qquad (6)$$

Few experimental data exist for higher electric fields, but there are theoretical models available, such as that shown in the inset of Fig. 3b [16]. This model predicts that the relative permittivity will drop rapidly and eventually saturate as the field increases.

A centered-finite difference method with a variable grid was used to calculate the field distribution around a sphere for a given applied potential and water thickness. The resulting equations were solved using the Newton–Raphson method. Solutions to Poisson's and Laplace's equations are shown in Fig. 3 for three different adlayer thicknesses. The potential distributions in Fig. 3a show that the potential is nearly constant in thin adlayers (dashed line). Conversely, the potential distribution for a thick layer drops rapidly near the tip surface, and does not change much at the vacuum interface (thick line). The potential is approximately constant in the regions where the dielectric response of water screens out the electric field. Fig. 3b shows the field distributions for the potential profiles in Fig. 3a. The field distributions have been normalized by the applied field, which is the value of the field for a given applied tip potential in the absence of a condensed layer of water:

$$E_o = \psi_t / \beta r_t , \qquad (7)$$

where β is the shape factor and r_t the tip radius. The shape factor is 1 for a sphere and ~ 5 for a conical emitter tip [6]. The field distributions each have two local maxima: one at the tip surface and one at the vacuum interface. In a thin layer the field at the tip is reduced, while in a thick layer the potential near the tip decreases faster than it would in a vacuum. The field at the vacuum interface approaches the applied field as the water layer thins. The thin line in Fig. 3b represents the conditions at which the field at the tip surface equals that at the vacuum interface.

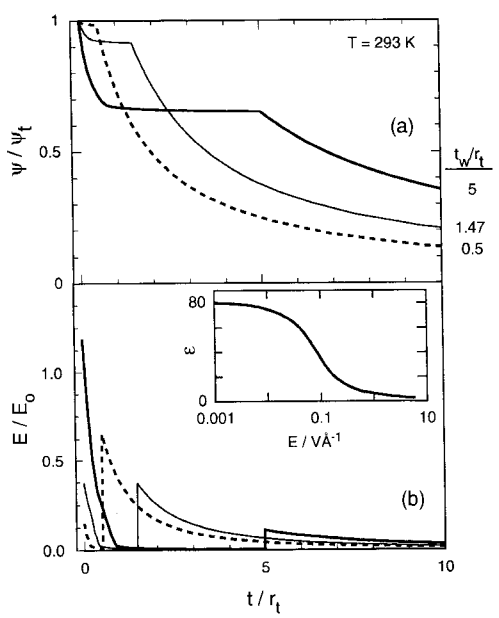

Fig. 3. Solutions to Poisson's and Laplace's equations at 293 K for a tip radius r_t and a tip potential ψ_t. The dashed line is the solution for a ratio of water thickness to tip radius (t_w / r_t) of 0.5, the thin line for a ratio of 1.47, and the heavy line for a ratio 5. (a) Dimensionless potential profiles, ψ/ψ_t, as a function of t/r_t, the ratio of distance from the tip to tip radius. (b) Calculated field distribution E normalized by the applied field E_o (Eq. (7)). The inset shows the field-dependent relative permittivity, ε used in the calculations [16]. The applied field E_o is the field at the tip surface in the absence of a water adlayer.

Fig. 4 shows how the electric fields at the vacuum and tip interfaces vary with applied field and water adlayer thickness for the field-dependent relative permittivity model shown in Fig. 3. The heavy line in Fig. 4 represents the conditions at which the fields at the tip (E_t) and vacuum (E_v) interfaces are equal (this condition is illustrated by the thin lines in Fig. 3). Fig. 4 shows that with increasing thickness at a constant applied field, the vacuum field decreases while the tip field increases. If the water adlayer is thin, then the tip field is weak and the vacuum field is slightly less than the applied field. In contrast, if the water adlayer is thick, then the tip field becomes dominant while the vacuum field is negligible. Thus, the amount of water adsorbed on the tip has a significant influence on the electric field distribution.

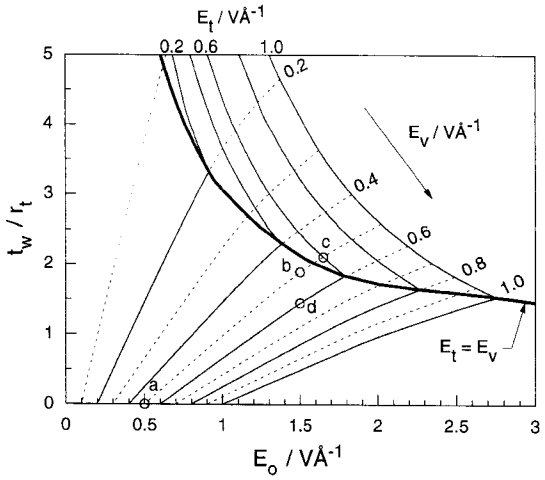

Fig. 4. Effect of water thickness t_w and applied field on the fields at the tip surface E_t and at the vacuum interface E_v for a tip of radius r_t. The applied field E_o is the field at the tip surface in the absence of a water adlayer (Eq. (7)). The heavy line represents the conditions at which E_t and E_v are equal. The circles are points discussed in Section 4. The numerical analysis is valid until the fields become sufficiently large to ionize water.

The predicted potential profiles vary from molecular dynamics (MD) predictions in three respects. First, MD simulations predict that the preferential orientation of the water molecules at the vacuum interface produces a field of 0.2 V Å^{-1} [17]. This contribution to the electric field is not included in our model. Second, MD simulations predict that the potential at an electrode surface exhibits strong oscillations which dampen significantly within two to three molecular diameters [18]. These oscillations are due to the finite size of the water molecules. Finally, MD simulations calculate larger fields at the electrode surface than our model for thin layers. For example, Nagy and Heinzinger calculate a field of 0.9 V Å^{-1} at the electrode surface for 20 Å of water between two platinum electrodes in a 1 V Å^{-1} external field [19]. Our continuum model predicts this field will be 0.015 V Å^{-1}. This is approximately the same as the average value Nagy and Heinzinger calculate 6 Å from the electrode surface. These differences in the calculated fields are not surprising because our model is not valid at the molecular level and does not include water–metal interactions. However, it does appear that our results compare well with MD calculations beyond two to three molecular diameters of the electrode/tip surface.

4. Equilibrium water thickness

As discussed previously, there is a direct correlation between pressure at condensation onset and electric field strength. The solid line in Fig. 2 represents the conditions at which multilayer condensation of water can begin. If the electric fields in Fig. 2 are taken to be the fields at the outermost layer of water, then the lines of constant vacuum field in Fig. 4 correspond to lines of constant chamber pressure. For example, Fig. 2 shows that water begins to condense at a vacuum field of 0.5 V Å^{-1} and a partial pressure of water of 1.1×10^{-3} Torr. This condition corresponds to point *a* in Fig. 4. Once a complete monolayer forms, the vacuum field drops below the field required for condensation and no more water forms on the tip. However, if the applied field is increased, then water will continue to grow on the tip. For example, if the applied field is increased to 1.5 V Å^{-1}, point *b*, the water formation will follow the constant vacuum field (or constant chamber pressure) line in Fig. 4, and the final water thickness will be 380 Å for a 200 Å tip.

As the applied field and/or water thickness continues to increase, either the vacuum field or the tip field will become sufficiently large to cause ionization. At this point our model is no longer valid. However, if the fields at which ionization occur are known, then our model can be used to predict the onset of ionization.

Water ionizes through two mechanisms: chemical ionization and electronic ionization. The mechanism for chemical ionization is [20]:

$$(H_2O)_{m+n+1} \rightarrow (H_2O)_m \cdot OH^- + (H_2O)_n \cdot H^+ \quad (8)$$

and that of electronic ionization is:

$$H_2O \rightarrow H_2O^+ + e^- . \quad (9)$$

Schmidt observed two modes of ionization in his experiments [7]. Ionization in condensed water occurred at 0.2 and 0.61 V Å^{-1} for tungsten and platinum, respectively. As discussed previously, the strong substrate dependence in these data may be

due to partial surface coverage. The field at which ionization occurs in a thick water layer has not been determined. It is unclear whether the ionization mechanism in the condensed layer is chemical or electronic. Schmidt reports that electronic ionization occurs in the gas phase at a field of 1 V Å^{-1}.

Fig. 4 can be used to determine the conditions at which water starts to ionize. For example, if water ionizes at 0.6 V Å^{-1}, then ionization will occur at the tip surface at a partial pressure of water of 1.1×10^{-3} Torr ($E_v = 0.5$ V Å^{-1}) and an applied field of 1.65 V Å^{-1}, as indicated in Fig. 4, point *c*. In contrast, if the applied field is held at 1.5 V Å^{-1} while the water pressure is reduced from 1.1×10^{-3} to 1.8×10^{-4} Torr, then the water layer will thin and the vacuum field will increase from 0.5 to 0.6 V Å^{-1} as shown in Fig. 4, point *d*. At this point, water will start to ionize at the vacuum interface. Thus, depending upon the water thickness and the applied field, the water adlayer will either ionize at the tip surface or at the vacuum interface.

Ramped field desorption experiments conducted by Stintz and Panitz may provide evidence for ionization at both the tip surface and the vacuum interface in water adlayers. In these experiments, water was dosed onto a tip in the absence of an applied field at cryogenic temperatures. The potential was then ramped until water started to ionize [21]. Stintz and Panitz found that ions desorbed from the tip in a controlled manner and that the applied field for ionization onset increased with water thickness. As can be seen in Fig. 4, this is the expected trend for ionization at the vacuum interface because this mode of ionization occurs at constant vacuum field.

In another set of experiments, Stintz and Panitz observed sporadic ion emission, rather than controlled desorption, when the water thickness exceeded a critical value [22]. The sporadic ion emission could indicate the formation of ions at the tip surface because embedded ions in the water adlayer may lead to a desorption process that cannot be easily characterized. More experimental data are required to verify the feasibility of determining the ionization location in the adlayer.

Ionization will occur at the location that has the highest electric field. Whether the tip or vacuum field dominates depends upon the applied field and the thickness of the water adlayer, as shown in Fig. 5. For thin films the vacuum field dominates, for intermediate films the tip field exceeds the vacuum field, and for thick films the tip field exceeds the applied field. The amplification of the tip field is due to the field dependence of the relative permittivity. If a constant permittivity model is used, the tip field never exceeds the applied field.

The results discussed in this Letter are similar to those of groups studying tunneling rates through dielectric films. Continuum models that assume the relative permittivity is constant, predict the tunneling rate through dielectric films is less than the tunneling rate in the absence of a dielectric layer [23]. These results are in stark contrast with underwater STM studies which show that water reduces the barrier to tunneling [24]. Benjamin et al. [25] have obtained qualitative agreement with these STM experiments by more accurately modeling the polarization, or relative permittivity, of water. Their molecular dynamics calculations predict that water significantly increases the tunneling probability, i.e., it increases the local field at the metal/water interface. A key difference between the results discussed herein and those of Benjamin et al. is that they show that the field at the metal/water interface is enhanced for thin layers of water while our model predicts this enhancement only for thick layers of water. This difference is most likely due to the fact that their calculations include the effects of metal–water interactions and our calculations neglect these effects.

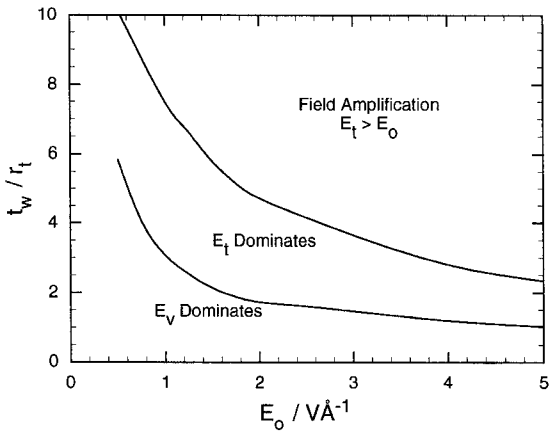

Fig. 5. Dependence of the dominant field on applied field E_o and the ratio of the water thickness to the tip radius, t_w / r_t. Field amplification occurs for thick adlayers and is characterized by the field at the tip surface becoming larger than the applied field.

5. Conclusions

The proposed numerical model can be used to study the trends in tip and vacuum fields as a function of pressure and applied field. The thickness is strongly dependent upon the partial pressure of water, the applied field, and the onset of ionization. The presence of the water adlayer can significantly change the electric field distribution around the tip. Thin water layers reduce the electric field at the tip surface while thick water layers tend to concentrate the electric field. The amplification of the tip field is due to the use of a field-dependent permittivity model. Depending upon the experimental conditions, water can ionize at either the tip surface or the vacuum interface. Future work will be focused on acquiring experimental verification of the proposed model.

Acknowledgements

We gratefully acknowledge support of this work from the Office of Naval Research. DLS is thankful for an Intel Foundation Graduate Fellowship.

References

[1] D.M. Kolb, C. Franke, Appl. Phys. A 49 (1989) 379.
[2] J.H. Block, in: R. Vanselow, S.Y. Tong (Eds.), Chemistry and Physics of Solid Surfaces, CRC Press, Cleveland, OH, 1977, p. 49.
[3] M.G. Inghram, R. Gomer, Z. Naturforsch. 10a (1955) 863.
[4] A.R. Anway, J. Chem. Phys. 50 (1969) 2012.
[5] T.T. Tsong, J. Vac. Sci. Technol. B 3 (1985) 1425.
[6] R. Gomer, Field Emission and Field Ionization, Am. Inst. Phys., New York, NY, 1993.
[7] W.A. Schmidt, Z. Naturforsch. 19a (1964) 318.
[8] H.D. Beckey, Principles of Field Ionization and Field Desorption Mass Spectrometry, Pergamon, New York, NY, 1977.
[9] M.A. Omar, Elementary Solid State Physics, Addison-Wesley, Reading, MA, 1975.
[10] T.T. Tsong, Atom-Probe Field Ion Microscopy, Cambridge University Press, New York, NY, 1990.
[11] C.P. Smyth, Dielectric Behavior and Structure, vol. 1, McGraw-Hill, New York, NY, 1955.
[12] D.R. Lide (Ed.), Handbook of Chemistry and Physics, 71st ed., CRC Press, Boca Raton, FL, 1990.
[13] T.D. Pinkerton, personal communication.
[14] K. Griffiths, R.V. Kasza, F.J. Esposto, B.W. Callen, S.J. Bushby, P.R. Norton, Surf. Sci. 307–309 (1994) 60.
[15] H.A. Kolodziej, B.P. Jones, J. Chem. Soc., Faraday Trans. II 71 (1975) 269.
[16] H.P. Huinink, A. de Keizer, F.A.M. Leermakers, J. Lyklema, J. Phys. Chem. 100 (1996) 9948.
[17] E. Spohr, J. Chem. Phys. 107 (1997) 6342.
[18] W. Schmickler, Chem. Rev. 96 (1996) 3177.
[19] G. Nagy, K. Heinzinger, Conf. Rec. 10th Int. Conf. on Conduction and Breakdown in Dielectric Liquids, IEEE, New York, 1990, p. 228.
[20] L. Onsager, J. Chem. Phys. 2 (1934) 599.
[21] A. Stintz, J.A. Panitz, J. Appl. Phys. 72 (1992) 741.
[22] A. Stintz, J.A. Panitz, Surf. Sci. 296 (1993) 75.
[23] P. Nordlander, J.P. Modisette, Nucl. Instrum. Methods, Phys. Res. B 135 (1997) 305.
[24] A. Mosyak, A. Nitzan, R. Kosloff, Chem. Phys. 104 (1996) 1549.
[25] I. Benjamin, D. Evans, A. Nitzan, J. Chem. Phys. 106 (1997) 6647.